

Journal of Materials Chemistry A

Accepted Manuscript



This is an *Accepted Manuscript*, which has been through the Royal Society of Chemistry peer review process and has been accepted for publication.

Accepted Manuscripts are published online shortly after acceptance, before technical editing, formatting and proof reading. Using this free service, authors can make their results available to the community, in citable form, before we publish the edited article. We will replace this *Accepted Manuscript* with the edited and formatted *Advance Article* as soon as it is available.

You can find more information about *Accepted Manuscripts* in the [Information for Authors](#).

Please note that technical editing may introduce minor changes to the text and/or graphics, which may alter content. The journal's standard [Terms & Conditions](#) and the [Ethical guidelines](#) still apply. In no event shall the Royal Society of Chemistry be held responsible for any errors or omissions in this *Accepted Manuscript* or any consequences arising from the use of any information it contains.

Harvesting heat energy from hot/cold water by using pyroelectric generator

Cite this: DOI: 10.1039/x0xx00000x

Qiang Leng, Lin Chen, Hengyu Guo, Jianlin Liu, Guanlin Liu, Chenguo Hu*, Yi Xi*

Received 00th xxx 2014,
Accepted 00th xxx 2014

DOI: 10.1039/x0xx00000x

www.rsc.org/

Waste heat has been regarded as one of the most important renewable and green energy sources under the threat of the global warming and energy crisis. In this work, we design a pyroelectric generator based on a polyvinylidene fluoride film for harvesting heat energy from hot/cold water which widely exists in industrial processes. To achieve practical application, the device simply contacts a hot flow and cold flow alternatively. The output open-circuit voltage and short-circuit current are up to 192 V and 12 μA , respectively, under the temperature change of 80 °C. The output power density can reach 14 $\mu\text{W}/\text{cm}^2$ that is a great improvement for the thermoelectric devices. The prepared pyroelectric generator can drive 42 green light-emitting diodes or charge a commercial capacitor (100 μF) to 3.3 V in 90 s. This work provides a promising strategy for efficiently harvesting waste heat from ambient and presents significant progress in thermoelectric conversion technology.

Introduction

Due to the threat of worldwide energy crisis, more and more scholars focus on exploring new energy resources. Waste heat utilization has attracted extensive attention and interest on account of its universality, availability and environmental friendliness. The internal combustion engines in cars produce much heat being scattered in the environment. Much cooling industrial waste water is directly discharged into the rivers along with the heat loss. Household water also contains much heat energy. If this waste heat could be harvested and utilized, it would be a great energy source.

Conventional solid-state thermoelectric technology uses electrons or holes as the working fluid for heat pumping and power generation based on Seebeck effect and offers the thermal-to-electrical energy conversion technology for generating electricity from waste heat.¹⁻³ A steady temperature gradient must be maintained in order to generate sustainable electricity. However, in an environment where the temperature would be spatially uniform without a gradient according to the principle of increase of entropy, it is difficult to achieve large difference of temperature in the ambient. Moreover, the thermal-to-electrical energy conversion efficiency based on the commercial thermoelectric materials is still very low.⁴

One of the least-known properties of solid materials, pyroelectricity is rigorously defined as the temperature dependence of the spontaneous polarization in certain anisotropic solids.^{5,6} The spontaneous polarization dipole moment is always nonzero in a pyroelectric material and is equivalent to a layer of bound charge on

each flat surface of the pyroelectric thin film. The feature of pyroelectric effect shows the net dipole moment (or bound charge) change with temperature variation that can be measured as an electric current from external circuit.

The devices based on pyroelectric materials have many advantages, such as easy integration with on-chip circuitry, uncooled detection, room-temperature operation, high speed, low system cost, portability and wide spectral response with high sensitivity. These devices have been successfully used in many applications, such as pollution monitoring, hot image detector devices, intruder alarms and gas analysis.⁷⁻¹⁰ However, pyroelectricity has often been abandoned as a practical energy source due to its low efficiency.¹¹ Recently, pyroelectric energy conversion has attracted more attention.¹² A. Cuadrada, et al. report a pyroelectric cell that can produce electricity from cyclic temperature fluctuations and charge 1 μF capacitor to supply low-power autonomous sensors.¹³ Z. L. Wang's group fabricates pyroelectric nanogenerators based on ZnO nanorod arrays, KNbO₃ nanorods and lead zirconate titanate film, and hybrid energy cell for simultaneously harvesting thermal, mechanical and solar energy.^{14,15} However, the output voltage and current for the pyroelectric cells or generators based on inorganic pyroelectric materials are still relatively low (voltage below 22 V, and current below 170 nA).¹⁶ Then an organic polyvinylidene fluoride (PVDF) has been recently used for pyroelectric nanogenerator¹⁷ due to its promising pyroelectric properties with a pyroelectric coefficient up to 200 $\mu\text{C m}^{-2}\text{K}^{-1}$.¹⁸⁻²² Although it just works as one part for harvesting energy in hybrid energy cell, it reveals the outstanding pyroelectricity of PVDF.

The thermal sources to produce time-dependent temperature variations (dT/dt) of all the energy produce devices based on pyroelectric effect depend on electrical heaters.^{14-16, 22-24} However, it is not really energy from environment. Until now, there has been no report on pyroelectric generators which harvest heat energy simply from hot/cold water.

In this work, we made a pyroelectric generator (PEG) based on a PVDF film for harvesting heat energy from hot/cold water which widely exists in industrial processes, such as oil refining, steel making and glass making or produced by nature such as geothermal heat, volcano heat and solar heat. Hot water can be obtained from solar energy water heaters daily in every house. To achieve practical application, the device simply contacts a hot flow and cold flow alternatively to produce time-dependent temperature variations. Although the periodic moving device to contact hot and cold flow is driven automatically by an electric oscillator, this driving force would be replaced by water flow after some mechanical design, such as ancient water mills. The output open-circuit voltage and short-circuit current are up to 192 V and 12 μA respectively under the temperature change of 80 °C. The output power density can reach 14 $\mu\text{W}/\text{cm}^2$ that is a great improvement for the thermoelectric devices. The prepared pyroelectric generator can drive 42 green light emitting diodes (LEDs) or charge a commercial capacitor (100 μF) to 3.3 V in 90 s. Compared to other nanogenerators, including piezoelectric nanogenerators based on pressure or bending,²⁵⁻²⁸ or triboelectric nanogenerators used to harvest airflow energy,^{29,30} vibration energy,^{31,32} and rotary energy³³, our pyroelectric generator provides a promising strategy for efficiently harvesting waste heat from ambient and presents significant progress in thermoelectric conversion technology.

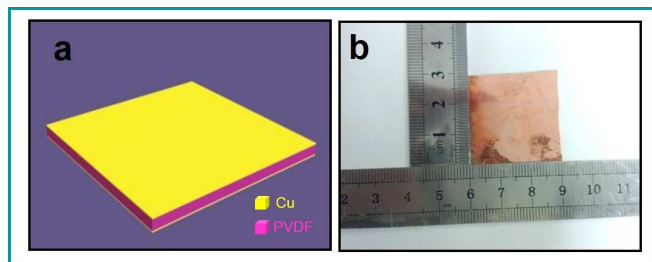


Figure 1. Schematic diagram (a) and digital photography (b) of a pyroelectric generator based on the PVDF film.

Experimental

The PVDF film with the thickness of 110 μm was purchased from Measurement Specialties (US). A 10 μm -thickness layer of copper was sputtered onto each side of the PVDF film as is shown in **Figure 1**. The Cu layers on the PVDF film worked as electrodes. Two Cu wires were fixed on the surfaces of the top and bottom Cu layers by the silver paste to link the device to the external instrument. To ensure the stability of the contact of the Cu layer and Cu wire, a kind of epoxy AB adhesive was covered on the joint. Then, a polyvinyl chloride (PVC) thin film with thickness of 30 μm covered on the whole device to proof the water which is usually conductive. The commercial capacitor in the charging experiment is an aluminum electrolytic capacitor (100 μF , 16 V) with the package size of 25 mm \times 25 mm.

The hot/cold flows were pumped to flow through two plastic tubes and then let the water drop down. The film of the PEG was

parallel to the water flows in working process. Two thermoelectric couples were used to monitor the temperature of the hot/cold flow. The PEG was alternatively driven to contact the hot flow and cold flow, respectively, by an electric oscillator (JZK-5). All the output current was measured by the current preamplifier (Stanford Research SR 570).

Results and discussion

As is shown in **Figure 1a**, the key part of pyroelectric generator (PEG) mainly contains three layers. Two thin layers of Cu work as top and bottom electrodes, respectively. The PVDF film acts as the pyroelectric material. From **Figure 1b**, the length and width of the device is about 30 mm \times 30 mm. The thickness of PVDF film is 110 μm and the deposited Cu layer is about 10 μm . Good conductivity of Cu helps transfer induced electrons from the polarization fluctuation of the PVDF film to the external circuit effectively. In order to rapidly transport heat from water to the PVDF film to change its polarization state, the Cu layers should be thin enough. The device simply contacts the hot flow (40, 60, 80 °C) and cold flow (0 °C) alternatively to harvest heat energy from them.

Figure 2 illustrates our experiment setup. Two pumps are used to lift the cold and hot water to a higher level. The distance between two flows is about 3~4 cm. The device is driven to left and right by an oscillator in order to contact the flows (**Figure S1**). Once the device contacts the flow, there is an instantaneous current signal. Insets in **Figure 2** give the photographs of contacting cold flow (1) and hot flow (2) of the PEG and the lighted LEDs by its output power. The method of harvesting waste heat energy from hot water is an innovation in the development of the pyroelectric generators.

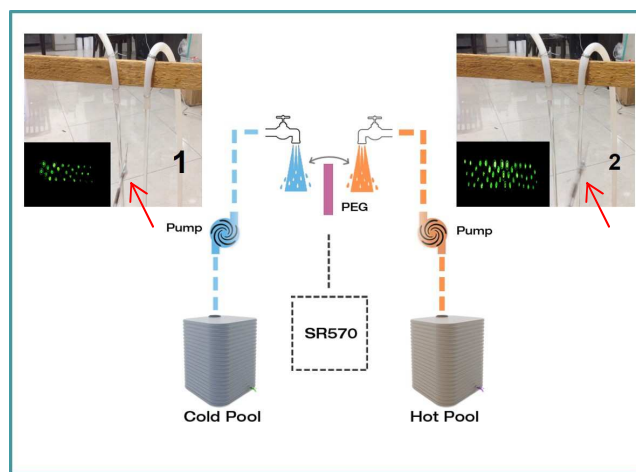


Figure 2. Experimental setup of the PEG under the alternative contact of the hot and cold water flow. Insets are the photographs of contacting cold flow (1) and hot flow (2) of the PEG and the lighted LEDs.

Figure 3a shows the generated short-circuit current under temperature difference of 40 °C between the hot flow and the cold flow. When the PEG contacts the hot flow, positive current peaks are detected. Negative current is detected when the PEG contacts the cold flow. And the maximum value of current is 5.79 μA . To investigate the effect of the temperature differences on the output current, we conduct another two experiments under the temperature differences of 60 °C and 80 °C, respectively. The corresponding output currents are shown in **Figure 3b** and **3c**. Obviously, with the increase in the temperature of the hot flow, the current increases.

Under the temperature difference of 80°C, the current reaches the maximum about 11 μA (Figure 3c). We notice the asymmetric current responses in Figure 3 where the current peaks always have a cleaner and faster response when the PEG is switched from the hot flow to cold flow (seen as the rapid change from positive peak to negative one). These asymmetric current responses are caused by the different mechanical vibrations when the PEG is switched from the hot flow to cold flow, which can be avoided by manual switch as is shown in Figure 4a.

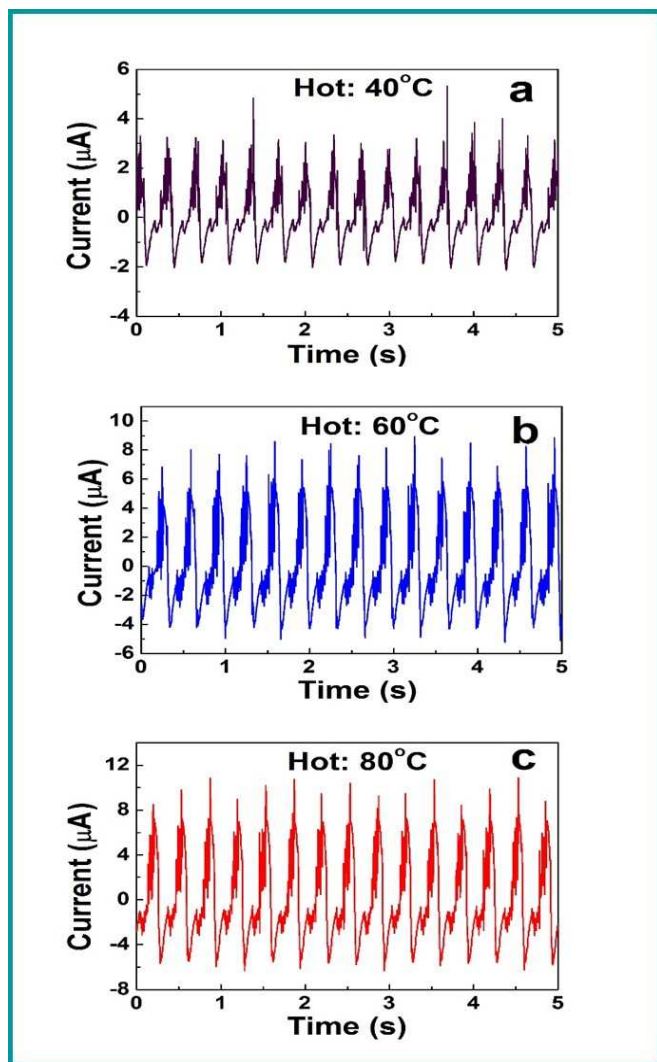


Figure 3. The output current of the PEG under the alternative contact of the cold flow at 0°C and the hot flow at 40°C (a), 60°C (b) and 80°C (c), respectively.

In order to guarantee the sufficient contact of the PVDF film with the hot or cold flow, we manually control the device to contact the hot water and the cold water alternatively in two beakers (Figure S2 and Video 1). Figure 4a shows the output current versus time when the PEG contacts the hot and cold flows periodically. The whole period from contact to separation between hot and cold flows is actually about 1.4736 s, which can be counted from the recorded data in Figure 4a. We enlarged one period to see the details as is shown in Figure 4b. Once the device contacts the hot water (80°C), the temperature of the PVDF film immediately rises with rapid

increase of current from zero to the peak within 0.05 s which also can be seen from Figure S3.

Generally, the pyroelectric current I can be determined by the equation

$$I = pAdT / dt \quad (1)$$

where p , A and dT/dt are the pyroelectric coefficient, effective area of the device and rate of change in temperature, respectively.^{15,34} In this work, the time for the device to contact the hot flow or cold flow is quite short. Thus, the real temperature of the PVDF film cannot be

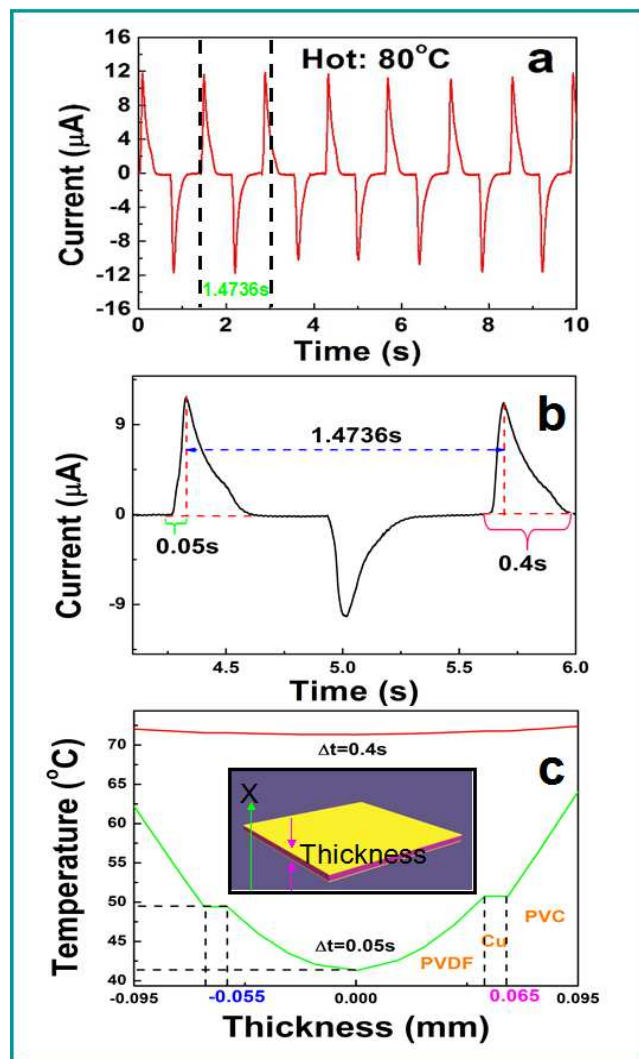


Figure 4. The output current under manual operation (a). The enhanced one period of the current signal (b). The temperature distribution across the thickness of the device at 0.05s and 0.4s (c).

the same as that of the hot flow or cold flow instantaneously. We assume that the temperature around the surface of the PVDF film rises or drops to a certain temperature between those of the hot flow and cold flow. The temperature on the PVDF is also simulated using Comsol Multiphysics software. Before the device sinks into the hot water, the temperature of the PVDF film is equal to that of the room temperature (20°C). Then it increases up rapidly after the device sinks into the hot water. The temperature distribution in the cross-section of the PVDF film is shown in Figure 4c, from which we can apparently see the temperature change at the moment when the

device is put into hot water (80°C). In the cross section, the PVDF film with a thickness of 110 μm is covered by 10 μm Cu layer on both surface, and the Cu layer is covered by PVC with thickness of 30 μm . The temperature across the thickness is not uniform as the PVDF film has a thickness of 110 μm . Because of the symmetry of the device, we set film thickness along X direction and $X=0$ in the middle of cross-section. The temperature at $X=0$ plane is the lowest and the film surface is the highest. Then the temperature at $X=0$ plane and the surface is chosen to calculate the output current, respectively. Then the corresponding current values are 11.42 μA and 14.58 μA calculated by equation (1). The temperature distribution across the thickness when the device contacts cold water is also simulated as is shown in Figure S4.

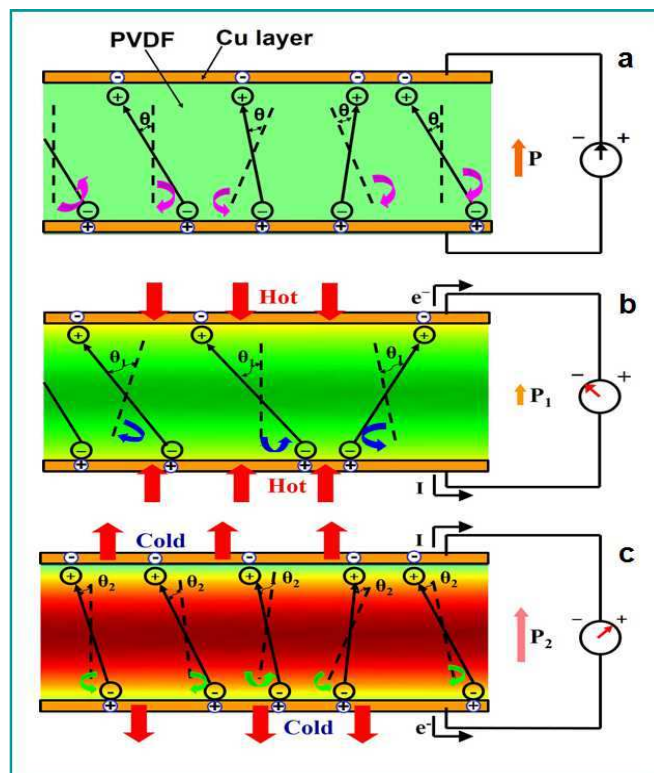


Figure 5. Schematic sketch of the pyroelectric generating mechanism. No output without temperature change (a), the bound charge change caused from the polarization state change and external current flow after contacting hot flow (b) and cold flow (c).

During this process, the temperature at the surface rises rapidly up to 50°C and then to 72°C. Subsequently, the device is taken out of the hot water and put into the cold water quickly. The PVDF film cools down instantaneously. The maximum temperature difference reaches 23.3°C at the moment when the device is inserted into the cold water (0°C) as is shown in Figure S4. Using equation (1), we work out the maximum output currents are 14.58 μA and 11.32 μA , respectively when contacting hot water and cold water. The results are close to those (12.58 μA and 11.23 μA) obtained in experiment in Figure 4a. The temperature difference and distribution of the PVDF film in the hot water of 60°C and 40°C are also simulated (Figure S5 and S6). By simulation and calculation, we have further verified the pyroelectric equation.

To illustrate the mechanism of the pyroelectric generator, the schematic sketch is presented in Figure 5. As molecule thermal

motion depends on temperature, the direction of molecule spontaneous electric dipole is greatly affected by molecule thermal motion. In idea situation, all dipoles of molecules would align along one direction without wiggling (vibration) back and forth in absolute zero. As the temperature increases, the dipoles would diverse in direction and wiggle around their respective pole axes due to the thermal motion. Therefore, the axis direction of dipoles is more diverse and the wiggling angle θ enlarges at higher temperature.^{15,22,35} The changes due to the thermal fluctuations in hot/cold water are shown in Figure 5. Figure S7 shows the relationship between the maximum wiggling distance and angle θ . No output current is observed as the spontaneous polarization is constant under invariable temperature (Figure 5a). When the device contacts the hot flow, as the temperature of the PVDF film increases rapidly, the electric dipoles oscillate within a larger angle θ_1 with respect to original angle θ ($\theta_1 > \theta$) which significantly reduces the intensity of spontaneous polarization. A flow of electrons from the top electrode to the bottom one is generated due to the decrease in the induced charges in the electrodes as is shown in Figure 5b. Conversely, when the device contacts the cold flow, the electric dipoles oscillate within a smaller angle θ_2 due to less active thermal motion. Thus, the polarization is remarkably enhanced, which increases the induced charges in the electrodes. Then a flow of electrons from the bottom electrode to the top one is detected as is shown in Figure 5c.

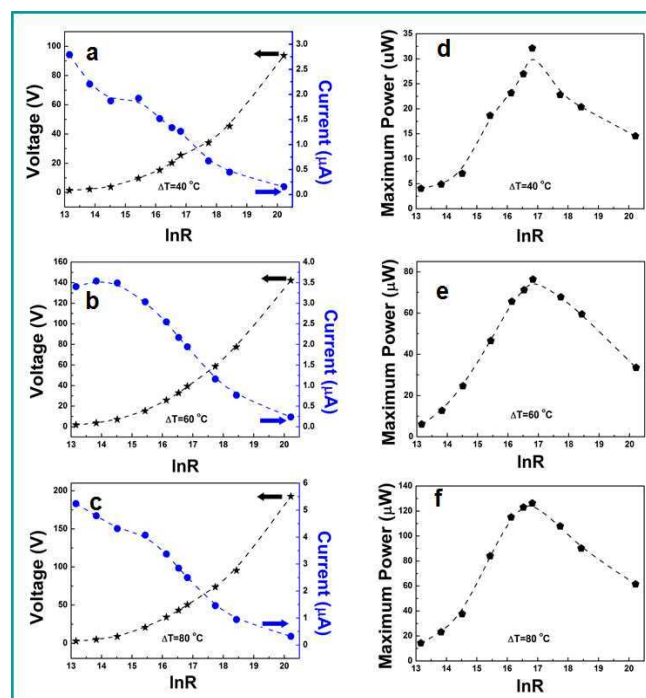


Figure 6. Output current and voltage and power of the PEG under temperature difference of 40°C (a, d), 60°C (b, e) and 80°C (c, f) between the hot flow and the cold flow. R means a load resistance.

However, as the PVDF is also a piezoelectric material, piezoelectric effect might contribute the output power by expanding/shrinking the film volume in varying temperature. To look into the origination of the piezoelectric and pyroelectric effects, both effects are caused by polarization dipole moment of molecules, which results in the bound charge variation on the surface of PVDF film. Therefore, the variation of polarization dipole moment of

molecules caused by temperature change can be all regarded as pyroelectric effect.

To study the conversion efficiency of the PEG, the output power is measured. **Figure 6** shows the output peak power, current and voltage as a function of load resistance for the PEG under various temperature differences. As the load resistance increases, the output current decreases, while the corresponding open-circuit voltage increases (**Figure 6a, 6b and 6c**). Moreover, as the temperature of the hot flow increases from 40 °C to 80 °C, the maximum open-circuit voltage increases from 93.6 V to 192.6 V accordingly. The output power firstly increases and then descends with the increase in the load resistance (**Figure 6d, 6e and 6f**). When the external load is 20 MΩ, the output power reaches the maximum of 32.1 μW ($\Delta T=40^\circ\text{C}$), 76.4 μW ($\Delta T=60^\circ\text{C}$) and 126.2 μW ($\Delta T=80^\circ\text{C}$), respectively. Similarly, the maximum output power increases as the temperature of the hot flow increases. These facts demonstrate that higher temperature difference generates larger open-circuit voltage, output current and output power, which are attributed to the enhancement of the change rate of spontaneous polarization under higher temperature difference. As far as we know, none of the previous pyroelectric generators can generate so high open-circuit voltage and output power, which is a result of the efficient heat transport for our device in hot/cold water.

In order to understand the high output voltage of the PEG, we simulate the electrical potential distribution of the PVDF film in the cross section under the alternative interaction of the hot flow at 80 °C and the cold flow at 0 °C by using the Comsol Multiphysics software. According to equation (1), the change of surface bound charge density can be expressed as

$$\Delta\sigma = I\Delta t / A = p\Delta T \quad (2)$$

Along the thickness of the PVDF film, the potential difference U between the top and bottom electrodes can be given by

$$U = Ed = \frac{\Delta\sigma d}{\varepsilon_r\varepsilon_0} = \frac{pd}{\varepsilon_r\varepsilon_0} \Delta T \quad (3)$$

Where E is the electric field intensity, d is the thickness of PVDF film, ε_r and ε_0 are the relative and vacuum dielectric constants respectively. In the simulation, the top Cu layer is connected to ground and the pyroelectric coefficient (p) of the PVDF film is 2.7 nC/cm²K.^{36,37} The electrical potential distribution can be observed in the cross-section of the PVDF film in which the maximum potential is about 774 V as is shown in **Figure 7a**. In our work, the maximum output voltage is about 192 V which is smaller than that of the simulation. As the PVDF film does not fully contact with the flows (**Figure S1**), there is a difference between the experimental data and the simulated result. In order to isolate the device from water, the PVC thin film attached on the surface of the device would affect the transmission of heat. The information of the PVC film is presented in **Figure 4c**.

However, PVDF is also a kind of piezoelectric material.^{38,39} To eliminate the piezoelectric effect of the PVDF film caused by the mechanical beating of the water flow, a comparative experiment is performed. We use the flows in the ambient temperature to replace both the hot flow and cold flow in which the PEG moves between the two flows without temperature difference. The output current is depicted in **Figure 7b**, indicating that the current generated from

piezoelectric effect is about 1~2 μA. Compared with the output current above, we demonstrate that the pyroelectric effect plays a leading role in this work.

Besides the temperature differences, we study the contact frequency of the device. **Figure 8a-8f** show the output current at different contact frequency (left) and the quantity of charge transfer in half a cycle per second (right) of the PEG under various temperature differences. It reveals that the output current increases as the contact frequency increases. After reaching the maximum at the frequency of 5 Hz, the current begins to decrease because the time for the PDVF film to contact the flow decreases with the increases in contact frequency. Although the temperature difference in the PDVF between hot-cold contacts may reduce with increase in frequency, the reduction is not large enough to reduce the temperature change rate due to the good heat conductivity of the Cu

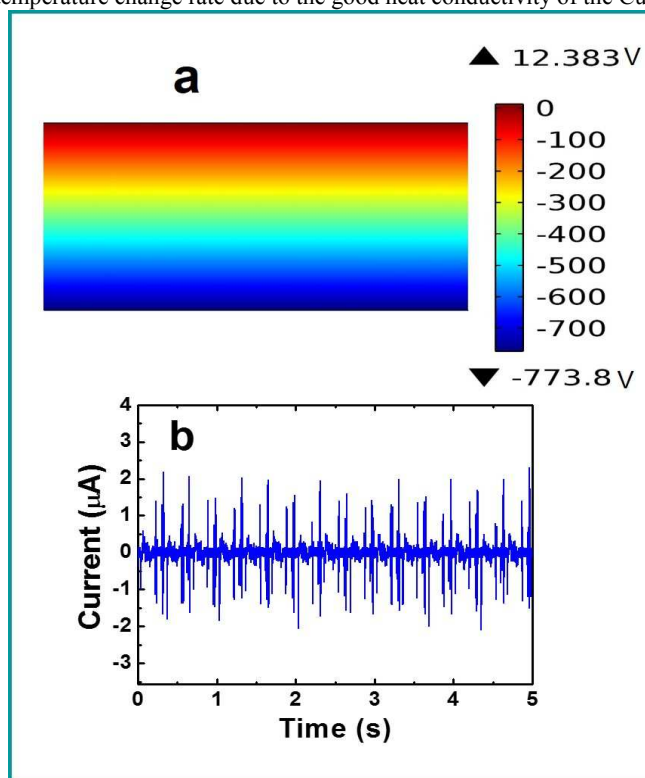


Figure 7. (a) The simulated electrical potential distribution along the thickness of the PVDF film. (b) The current induced by the piezoelectric effect of the PVDF film.

layer. Consequently, the output current is enhanced as the rate of temperature change rises sustainably (<5 Hz). However, if the frequency is higher than 5 Hz, not much heat could transfer from the flow to the PVDF film within a short contact time and then the temperature change rate decreases. Thus, the output current decreases gradually with the increase in the contact frequency of the device. Comparing **Figure 8b, 8d and 8f**, the quantity of charge transfer increases as the temperature difference increases due to the enhancement of the output current, especially under the hot flow of 60 °C and 80 °C. Particularly, the quantity of charge transfer per second under the hot flow at 80 °C is 4.52 μC at 7 Hz, which reveals the potential application in charging storage devices such as Li-ion batteries and capacitors. The detail calculation of charge transfer quantity per second is shown in **Figure S8**.

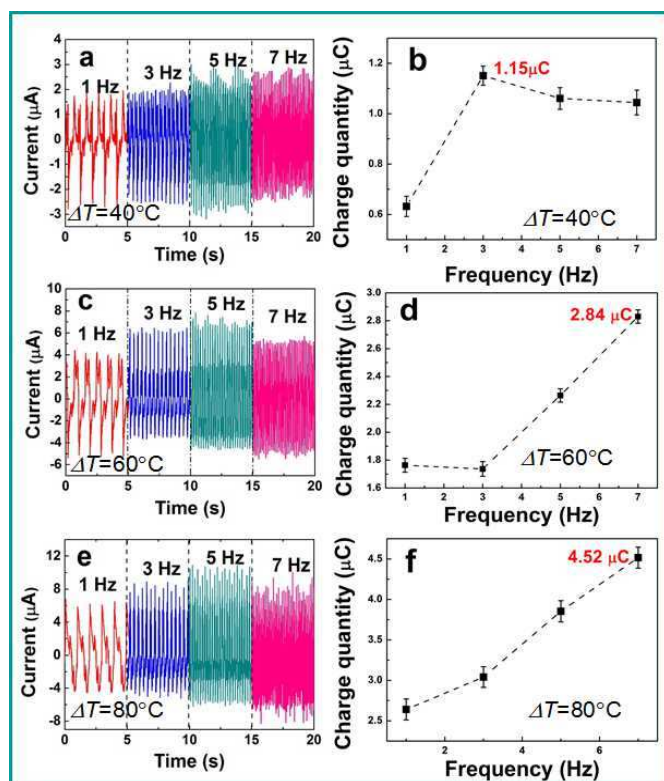


Figure 8. Output current at different contact frequency of the device and the corresponding quantity of the charge transfer per second at the temperatures of 40°C (a, b), 60°C (c, d) and 80°C (e, f).

To test the real output power and explore the potential application of the PEG, we use the PEG to drive LEDs directly. The LEDs in Line 1 are linked in series for receiving the forward output, while LEDs in Line 2 are linked in series for receiving the reverse output. The circuit is shown in Figure 9a. When the PEG contacts the hot flow (80°C), 42 LEDs in Line 2 are instantly lighting up and when the PEG contacts the cold flow (0°C), 26 LEDs in Line 1 are instantly lighting up. The photographs are shown in Figure 9b and 9c.

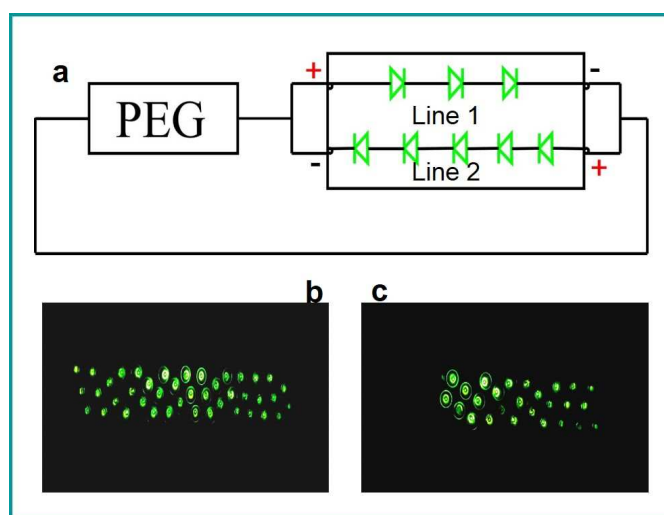


Figure 9. The equivalent circuit of powering LEDs (a). The optical images of lighting up LEDs when contacting hot flow at 80°C (b) and cold flow at 0°C (c)

The process of driving LEDs can be seen in **Video 2**. The current obtained from hot flow is larger than that from cold flow, which can also be seen from **Figure 3**. It reveals that the output signals really come from our PEG which just harvests energy from the hot flow and the cold flow in a simple method. We also use the hot flow of 60°C and 40°C to light up LEDs as are shown in **Video 3** and **Video 4**. However, we have not found a report of lighting up these numbers of LEDs by using pyroelectric devices.

According to the quantity of charge transfer described above, the PEG has the potential ability to store the electric energy generated from the temperature difference between hot flow and cold flows into a storage device such as capacitors. We choose a commercial capacitor (100 μF) for charging test. The working frequency of the PEG is 5 Hz, and the temperature difference between the hot flow and the cold flow is 80°C. The equivalent circuit is illustrated in **Figure 10a**. **Figure 10b** shows the charging current-time signals within 20 s indicating that the charging current is slightly smaller than the short-current. **Figure 10c** gives the charging voltage-time curve of the capacitor, from which we can observe that the capacitor is charged from 0 V to 3.3 V in 90 s. The storage electric energy in the capacitor can drive a green LED (**Figure 10d**) for about 60 s. Figure 10e shows the optical image of the lighting LED.

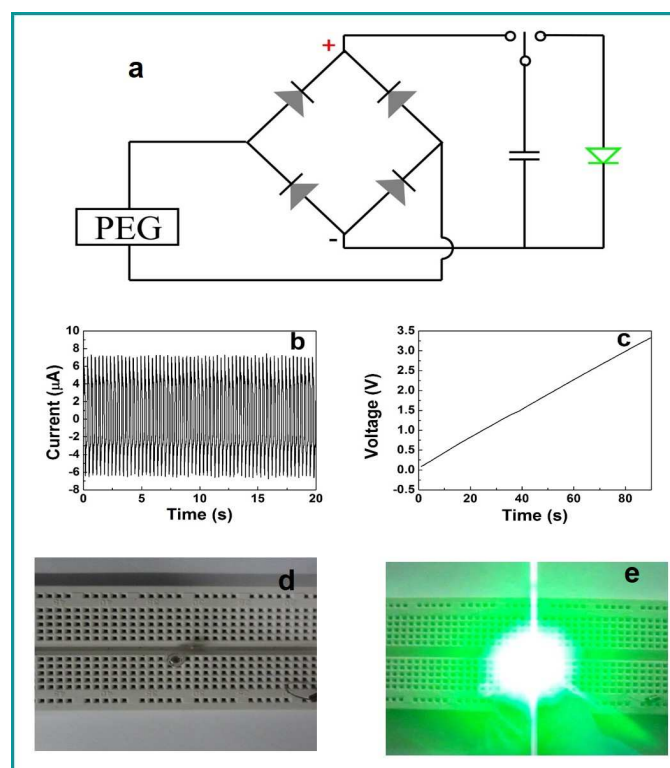


Figure 10. The equivalent circuit of charging a commercial capacitor (a). The time-current signals (b) and time-voltage curve (c) of the charging capacitor. The LED before (d) and after (e) being driven by the charged capacitor

Based on the investigations of directly driving LEDs and charging a capacitor to light up a LED, we can conclude that our PEG can effectively harvest energy from hot water and transfer thermal energy into electric energy. Moreover, the pyroelectric efficiency is relatively high compared with other devices. Our PEG may be applied to harvest energy from hot water in the factories and household water in the future.

Conclusions

In summary, we have designed and fabricated a pyroelectric generator based on the pyroelectric effect of the polyvinylidene fluoride (PVDF) film and successfully harvested thermal energy under the automatically alternative contact of the hot flow and cold flow. The working mechanism of the PEG is discussed in terms of polarization and thermal oscillation of the electric dipoles in the PVDF film. The temperature of the PVDF film before and after contacting hot or cold water is simulated to confirm the output current generated from the PEG. The calculated result is quite close to the experimental result. The output open-circuit voltage and short-circuit current are up to 192 V and 12 $\mu\text{A}/\text{cm}^2$ respectively under the temperature change of 80°C. The out-put surface and volumetric power density can reach 14 $\mu\text{W}/\text{cm}^2$ (1.08 W/cm^3), which is a great improvement for the thermoelectric devices. In order to understand the high output voltage of the device, the electrical potential distribution across the PVDF film is simulated, in which the theoretic output voltage is higher than the experiment result, indicating that the output power could be improved further. The electric energy generated by the PEG can light up 42 LEDs when the device contacts the hot flow and it can be also used to charge a commercial capacitor (90 s, 3.3 V) to light up a green LED for 60 s. The present results suggest that the PEG could be potentially used in energy supply for energy storage devices and self-powered electronic devices.

Acknowledgements

This work is supported by the NSFCQ (cstc2012jjB0006), SRFDP (20110191110034, 20120191120039), NSFC (11204388), and the Fundamental Research Funds for the Central Universities (CDJRC10300001, CDJZR11300004, CDJZR12225501, CQDXWL-2013-012). Qiang Leng and Lin Chen contributed equally to this work.

Notes and references

Qiang Leng, Lin Chen, Hengyu Guo, Jianlin Liu, Guanlin Liu, Prof. Chenguo Hu, Prof. Yi Xi

Department of Applied Physics, Chongqing University
Chongqing 400044, P.R. China

E-mail: hucg@cqu.edu.cn (C. G. Hu); yixi6@cqu.edu.cn (Y. Xi)

- 1 F. J. DiSalvo, *Science* 1999, 285, 703-706.
- 2 L. E. Bell, *Science* 2008, 321, 1457-1461.
- 3 Y. Yang, Z.-H. Lin, T. Hou, F. Zhang and Z. L. Wang, *Nano Res*, 2012, 5, 888-895.
- 4 P. L. Hagelstein, Y. Kucherov, *Appl. Phys. Lett.* 2002, 81, 3.
- 5 C. P. Ye, T. Tamagawa and D. L. Polla, *J. Appl. Phys.* 1991, 70, 5538-5543.
- 6 J. C. Joshi, A. L. Dawar, *Phys. Stat. Sol.* 1982, 70, 353-369.
- 7 R. W. Whatmore, *Rep. Prog. Phys.* 1986, 49, 1335-1386.
- 8 S. G. Porter, *Ferroelectrics* 1980, 33, 193-216.
- 9 C. C. Chang, C. S. Tang, *Sens. Actual. A* 1998, 65, 171-174.
- 10 V. Ferrari, A. Ghisla, D. Marioli and A. Taroni, *IEEE Sens. J.* 2003, 3, 212-217.
- 11 E. Fatuzzo, H. Kiess, R. Nitsche, *J. Appl. Phys.* 1966, 37, 510-516.
- 12 Y. Yang, K. C. Pradel, Q. Jing, J. M. Wu, F. Zhang, Y. Zhou, Y. Zhang and Z. L. Wang, *ACS Nano*, 2012, 6, 6984-6989.
- 13 A. Cuadras, M. Gasulla, V. Ferrari, *Sens. Actuat. A* 2010, 158, 132-139.
- 14 Y. Yang, W. X. Guo, K. C. Pradel, G. Zhu, Y. S. Zhou, Y. Zhang, Y. F. Hu, L. Lin and Z. L. Wang, *Nano Lett.* 2012, 12, 2833-2838.
- 15 Y. Yang, J. H. Jung, B. K. Yun, F. Zhang, K. C. Pradel, W. X. Guo and Z. L. Wang, *Adv. Mater.* 2012, 24, 5357-5362.
- 16 Y. Yang, S. Wang, Y. Zhang and Z. L. Wang, *Nano Lett.* 2012, 12, 6408-6413.
- 17 Y. Yang, H. L. Zhang, G. Zhu, S. Lee, Z. H. Lin and Z. L. Wang, *ACS Nano* 2013, 7, 785-790.
- 18 J. G. Bergman, JR., J. H. McFee and G. R. Crane, *Appl. Phys. Lett.* 1971, 18, 203-205.
- 19 R. L. Peterson, G. W. Day, P. M. Gruzensky and R. J. Phelan, *J. Appl. Phys.* 1974, 45, 3296-3303.
- 20 J. H. McFee, J. G. Bergman and G. R. Crane, *Ferroelectric* 1972, 3, 305-313.
- 21 X. Li, S.-G. Lu, X.-Z. Chen, H. Gu, X.-S. Qian and Q. M. Zhang, *J. Mater. Chem. C* 2013, 1, 23.
- 22 J. H. Lee, K. Y. Lee, M. K. Gupta, T. Y. Kim, D. Y. Lee, J. Oh, C. Ryu, W. J. Yoo, C. Y. Kang, S. J. Yoon, J. B. Yoo and S. W. Kim, *Adv. Mater.* 2013, 03, 570-574.
- 23 R. B. Olsen, D. A. Bruno, J. Merv Briscoe, *J. Appl. Phys.* 1985, 58, 4709-4716.
- 24 H. Nguyen, A. Navid, L. Pilon, *Appl. Therm. Eng.* 2010, 30, 2127 - 2137.
- 25 X. D. Wang, J. H. Song, J. Liu and Z. L. Wang, *Science*, 2007, 316, 102-105.
- 26 S. Xu, B. J. Hansen and Z. L. Wang, *Nat Commun.*, 2010, 1, 93-97.
- 27 X. D. Wang, *Nano Energy*, 2012, 1, 13-24.
- 28 W. Z. Wu, Z. L. Wang, *Angew. Chem. Inter. Ed.*, 2012, 51, 11700-11721.
- 29 H. Y. Guo, X. M. He, J. W. Zhong, Q. Z. Zhong, Q. Leng, C. G. Hu, J. Chen, L. Tian, Y. Xi and J. Zhou, *J. Mater Chem A*, 2014, 2, 2079-2087.
- 30 C. L. Sun, J. Shi, D. J. Bayer and X. D. Wang, *Energy Environ. Sci.*, 2011, 4, 4508-4512.
- 31 H. L. Zhang, Y. Ya, Y. J. Su, J. Chen, K. Adams, S. Lee, C. G. Hu and Z. L. Wang, *Adv. Funct. Mater.*, 2014, 24, 1401-1407.
- 32 Y. F. Hu, J. Yang, Q. S. Jing, S. M. Niu, W. Z. Wu and Z. L. Wang, *ACS Nano*, 2013, 7, 10424-10432.
- 33 L. Lin, S. H. Wang, Y. N. Xie, Q. S. Jing, S. X. Niu, Y. F. Hu and Z. L. Wang, *Nano Lett.*, 2013, 13, 2916-2923.
- 34 S. B. Lang, S. A. M. Tofail and A. A. Gandhi, M. Gregor, C. Wolf-Brandstetter, J. Kost, S. Bauer and M. Krause, *Appl. Phys. Lett.* 2011, 98, 123703-123703-3.
- 35 N. T. Tien, Y. G. Seol, L. H. A. Dao, H. Y. Noh and N. E. Lee, *Adv. Mater.* 2009, 21, 910-915.
- 36 Z. Y. Feng, X. Y. Zhao and H. Luo, *J. Am. Ceram. Soc.* 2006, 89, 3437-3440.
- 37 R. W. Whatmore, *Rep. Prog. Phys.* 1986, 49, 1335-1386.
- 38 S. Choi, Z. W. Jiang, *Sensors and Actuators A* 2006, 128, 317-326.
- 39 J. Dargahi, R. Sedaghati, H. Singh and S. Najarian, *Mechatronics*. 2007, 17, 462-467.